HHS Public Access

Author manuscript

Radiol Clin North Am. Author manuscript; available in PMC 2016 January 25.

Published in final edited form as:

Radiol Clin North Am. 2011 July ; 49(4): 749–vii. doi:10.1016/j.rcl.2011.05.006.

Imaging pediatric bone sarcomas

Sue C. Kaste

Departments of Radiological Sciences and Oncology, St. Jude Children's Research Hospital, MSN #220, 262 Danny Thomas Place, Memphis, TN, 38105 and from the Department of Radiology, University of Tennessee School of Health Science Center, 910 Madison Avenue, Memphis, TN, 38163.

Keywords

osteosarcoma; Ewing sarcoma; chondrosarcoma; pediatric bone tumors

INTRODUCTION

Primary malignant bone tumors are rare (8.7 cases per million annual incidence), and account for about 6% of all new pediatric cancer cases per year in the United States[16]. Osteosarcoma and Ewings Sarcoma Family of Tumors (ESFT) comprise the majority of cases (400 and 250 cases per year, respectively)[78]. Patients typically present with pain and/or swelling. Identification of the lesion not uncommonly occurs as a result of imaging performed for trauma. Diagnosis is frequently delayed for several weeks to months due in part to the rarity of such tumors and that the presence of a malignancy in an otherwise healthy adolescent is unexpected. Continuous evolution of chemotherapy regimens, surgical techniques and imaging technology have contributed to improved overall survival. Thus, tumor management and patient care should be provided by a multidisciplinary team of healthcare professionals that includes radiology, oncology, orthopedic surgery, radiation oncology, and physical therapy[29].

Bone tumors are classified according to the proliferating cell type. Each of the elements of which bone is comprised – cartilage, osteoid, fibrous tissue and marrow – can give rise to benign or malignant tumors. Clinical and standard imaging (radiographs, 99m technetium methylene disphoshonate bone scans (99mTc-MDP), computed tomography) characteristics of the various tumor types have been previously published and have not appreciably changed over the decades[86;114]. However, imaging recommendations evolve in concert with treatment advancements and clinical trials regimens[83]. This chapter reviews the three most common pediatric bone sarcomas - osteosarcoma, Ewing sarcoma, and chondrosarcoma and

Corresponding author for proof and reprints: Sue C. Kaste, DO, Department of Radiological Sciences, MS #220, St. Jude Children's Research Hospital, 262 Danny Thomas Place, Memphis, Tennessee 38105, Phone: (901) 595-3347, Fax: (901) 595-3981, sue.kaste@stjude.org.

their imaging as applicable to contemporary disease staging and monitoring, and explores the roles of evolving imaging techniques such as magnetic resonance (MR) and PET-CT.

PEDIATRIC BONE SARCOMAS

Osteosarcoma

Osteosarcoma is the most common primary malignant bone tumor. It occurs primarily during puberty and has been associated with rapid patient growth[77]. In females, the peak age is earlier than in males (12 years versus 16 years, respectively)[77;85]. A second peak is seen in adults over 60 years of age. The reported incidence of osteosarcoma from the 2009 report from the Surveillance, Epidemiology, and End Results (SEER) Program is 4.4 cases per million in patients up to 24 years of age, more prevalent in blacks than whites (4.2 versus 5.0, respectively) and more prevalent in females than males.

The current 5-year relative survival rate of pediatric cases is 61.6 % [85]. Advances in therapy improved survival from 15 – 20% when surgery alone was used for therapy to 55-80% by the 1980's with the addition of chemotherapy[75;77]. However, no significant improvement in survival rates has occurred between 1994 and 2003[85]. Survival has been associated with age at diagnosis, race, anatomic site of the primary tumor (highest survival in bones of the hands or feet and poorest survival seen in pelvic primary tumors), pathologic subtypes (best in chondroblastic osteosarcoma and worst in small cell osteosarcoma), and stage of disease (localized disease best survival; those with distant metastatic disease the poorest) and response to chemotherapy[31;77;85] determined at the time of definitive tumor resection. Two-dimensional tumor size relative to the patient's body surface area[71] and/or absolute tumor size[62] may have prognostic roles.

Osteosarcoma is histologically composed of mesenchymal stem cells which produce osteoid. In addition to the ‘classical’ central medullary osteosarcoma, histologically distinct variants are also recognized - surface (parosteal, periosteal and high-grade) and low-grade intraosseous osteosarcomas[75;88]. With the exception of the high-grade surface osteosarcoma, these variants are associated with an overall more favorable prognosis.

Treatment is determined by tumor histology. Classical osteosarcoma is treated with neoadjuvant multiagent chemotherapy followed by surgery and additional chemotherapy[88]. Both parosteal and periosteal osteosarcoma require surgical resection. Chemotherapy is not typically indicated for parosteal osteosarcoma and its role in treating periosteal osteosarcoma is controversial[61]. As osteosarcoma is radiation resistant, radiation therapy is typically reserved for axial unresectable lesions and for palliative care[75]. The roles of vascular endothelial growth factor (VEGF)[91] and other signaling pathways are under investigation as potential factors to be integrated into risk-adapted therapy[72;91]. In response to the incorporation of new treatment agents into clinical regimens, the imaging assessment of the effectiveness of therapy must now reflect the biologic response of tumor with robust sensitivity and accuracy

Ewing sarcoma

Ewing sarcoma (a member of the Ewing sarcoma family of tumors) is the second most common malignant bone tumor in pediatrics[51;85;88]. These tumors are considered a small round blue cell tumor, thought to originate in neural crest cells[51]. Ewing sarcoma family of tumors is estimated to have an annual incidence in the United States of 2.1 cases per million children, accounting for about 2% of all pediatric and young adult cancers[51]. These tumors may arise in either bone or soft tissue, occur more frequently in males than in females and are associated with increased incidence in white and Hispanic children compared to black or Asian children[51]. The vast majority of ESFT cases are associated with a t[11;22] [q24;q12] translocation[16;51].

Several prognostic factors are considered in newly diagnosed patients with Ewing sarcoma. The recent SEER report based on over 1,600 cases of Ewing Sarcoma registered between 1973 and 2005, indicates that independently significant variables include distant disease stage, primary location of the axial skeleton, and primary tumor size exceeding eight centimeters as independent predictors of worse overall survival[57]. These investigators found no significant prognostic significance of race or age at diagnosis. However, amongst Caucasian patients, female sex was identified as an independent predictor of improved survival (p=.031)[57]. Notable is the incidence of Ewing sarcoma in Caucasians being nine times higher than in African Americans, and over the course of this study (1973-2005), the incidence of Ewing sarcoma increased only among Caucasians[57]. Pre-teens have improved outcome compared to adolescents, and both groups show improved survival when compared to adults[68]. Event free survival of patients with pelvic tumors has been reported to range from 43%[3] to50% compared with 61% in patients with proximal, 68% distal extremity primary tumors (p = 0.003)[45] and 60.6% extremity tumors in general[3]. More recently, Lin et al have demonstrated that centrally located primary disease (P=0.002) and tumor response to therapy (P=0.007) are independent predictors of local disease recurrence. Histologic response less than 90% necrosis was associated with increased risk of local disease recurrence[74]. Patients diagnosed with metastatic disease have a considerably worse outcome than those with non-metastatic disease and those with metastasis limited to the lungs fare better than those with either bone metastasis alone or both bone and lung metastasis as reported by the European Intergroup Cooperative Ewing Sarcoma Study Group[24]. As with the above factors, patients with larger tumors have a worse survival when compared with those with smaller tumors[5;45;68]. A more recent study of 21 pediatric patients who underwent both static and dynamic enhanced MR found tumor volume, width and depth, but not length or dynamic enhancement variables, at diagnosis correlate with the risk of metastatic disease[84].

Chondrosarcoma

Chondrosarcoma is a rare heterogeneous group of tumors that may arise from bone or soft tissue. Those arising from bone account for approximately 3.6% of all primary bone malignancies in the United States[20]. The incidence of chondrosarcoma is estimated to be 1/200,000/year with survival ranging from 0% to 93% depending upon histologic subtype[44]. From the National Cancer Data Base, Damron et al reported the 5-year relative survival of all forms of chondrosarcoma to be about 75% (range, 52% to 87% depending upon

histologic subtype)[25]. Survival over the past 30 years has remained static[44]. Prognostic predictors of outcome include grade and size of tumor and uncontaminated, wide surgical margins. The development of local disease recurrence also seems to portend development of distant metastases and ultimately poor survival[94]. These tumors have a predilection for the proximal femur and pelvis[98]. The incidence of chondrosarcoma increases with increasing age. Though most often seen in middle-aged patients, chondrosarcoma arises in adolescents and young adults as primary or secondary lesions.

In an estimated 0.5 to 5% of cases[10], chondrosarcomas may arise in a pre-existing lesion, most notably osteochondroma or enchondroma. Both the radiologic and histologic distinctions between a benign osteo- or enchondroma and malignant chondrosarcoma (grade 1) are difficult and associated with high interobserver variability[20;41;88;99]. Clinically, low-grade chondrosarcoma should be considered if a patient with enchondroma complains of pain, especially night pain[99]. Factors associated with increased risk of malignant dedifferentiation include the presence of multiple osteo- or enchondromas[47;88], axial location, size exceeding 5 cm[41]. Ahmed et al reported an institutional incidence of sarcomatous dedifferentiation of 7.6% in single osteochondromas and 36.3% in cases of multiple osteochondromas. They also found dedifferentiation of lesions to be associated with flat bone locations, male gender and developing in patients 10 to 20 years younger than primary chondrosarcoma[1].

Reported radiologic signs of sarcomatous dedifferentiation include heterogeneous mineralization, presence of a soft tissue mass, poorly defined lesion margination and destruction of the cartilaginous cap[1;76]. Several investigators have associated the presence of peritumoral edema with chondrosarcoma but not with enchondromas[1;22;55;56]. However, this association occurred in only 20% of cases of clear cell variant of chondrosarcoma reported by Janzen et al[56].

Clinical and radiologic techniques for differentiating between benign and malignant cartilaginous tumors are under development. Using the onset and rate of contrast enhancement, reports indicate a potential role for dynamic enhanced MR in differentiating between osteo- or endochondromas and chondrosarcomas but this technique was less helpful in patients whose growth plates were not yet fused[40]. Feldman et al have shown 18F-FDG to distinguish between benign enchondromas and chondrosarcoma with 90.9% sensitivity, 100% specificity and 96.6% accuracy when using maximum standard uptake values of 2.0 to distinguish between benign and malignant cartilaginous tumors[30]. However, the role of PET/PET-CT in differentiating between benign enchondromas and chondrosarcoma has not yet been established. Recent identification of integrin-linked kinase expression patterns may be able to serve as biomarkers capable of distinguishing between enchondromas and chondrosarcoma[90].

Chondrosarcomas are classified as grade 1-3, based upon clinical behavior and likelihood of metastasizing; central (arising from the intramedullary space) versus peripheral (arising from the surface of bone), and primary or secondary [20;47;99]. Between 85% and 90% of chondrosarcomas are classified as conventional chondrosarcoma[20;41;47], most of which are further classified as grade 1 or 2 (low- or intermediate grade) and behave in an indolent

manner with low potential to metastasize. The remaining 5-10% of conventional lesions are classified as grade 3 lesions and possess high metastatic potential[20]. Rare variants of chondrosarcoma include dedifferentiated chondrosarcoma; a low grade tumor which degenerates into a high-grade sarcoma. Mesenchymal chondrosarcoma accounts for about 3-10% of primary chondrosarcomas, is highly malignant, seen in a population younger than conventional chondrosarcoma and is associated with late local and distant disease recurrence[17;26;98]. The clear cell variant of chondrosarcoma accounts for about 2-5% of all chondrosarcomas, is seen in younger patients, has a predilection for involving the epiphysis of femur or humerus[22;98], and may clinically be confused with chondroblastoma[98]. Myxoid chondrosarcoma is a slow-growing tumor associated with frequent local recurrence and metastases; it is seen in younger patients[20;26]. Periosteal chondrosarcoma is a very rare form which accounts for less than 2% of chondrosarcomas. Unlike the lesions discussed above, this variant arises from the cortical surface, most commonly of the metaphysis[18], and is covered by a fibrous sheath that is contiguous with the periosteum[18;41;86]. As it typically is found in patients in the second to fourth decades of life, these lesions may be seen in adolescents; there is a predilection for males[18].

Overall, the prognosis for patients with chondrosarcoma is favorable. From nearly 3000 cases captured in the SEER database, only tumor grade and stage were found to be independent predictors of for survival. Patients surviving 10 years from diagnosis were unlikely to die of disease related causes[44]. Surgical resection the primary means of local tumor control[26;47]. Prognosis and the likelihood of local recurrence, are correlated with the adequacy of surgical resection[99;111]. Radiation therapy may be useful for treatment of positive surgical margins, but its role has been controversial in treating chondrosarcoma because of the relative resistance of the tumor to radiation therapy[111]. Chemotherapy for advanced or metastatic disease and its utility in variant forms of chondrosarcoma has been of inconsistent value[41;98;99]. As these tumors are relatively resistant to radiation therapy, development of novel therapies is needed to improve disease control, particularly in cases of metastatic disease[47]. Recent genetic and molecular biologic studies have identified a variety of gene expressions, signaling pathways, receptors, oncogene mutations and hormones that may provide targets for development of novel and specific therapeutic targets[10;20;91;101;115].

THE ROLE OF IMAGING

Diagnostic imaging provides information critical to local disease staging, identification of distant metastases, monitoring response to therapy and detecting recurrent disease. Imaging techniques which adhere to the ALARA (as low as reasonably achievable) must be utilized that optimize the accuracy of diagnosis and staging while minimizing patient exposure to ionizing radiation[46;64;92;102;109]. Initial evaluation is based upon radiographs. MR is typically performed following demonstration of a bone tumor; definitive diagnosis requires histologic analysis.

Staging work-up of the primary tumor should ideally be performed prior to biopsy for several reasons[13;83;114]. Post-operative changes can complicate imaging interpretation, and therefore, the usefulness of postoperative imaging as staging information may be limited. Biopsy is directed by imaging and the biopsy approach should be coordinated with the

surgical approach planned for the definitive surgical procedure. Such a practice limits the risk of contaminating soft tissues with tumor cells in a region that would not ordinarily be resected. Biopsy from an approach not included in the planned surgical field risks expanding the volume of tissues ultimately requiring surgical resection[29]. An incisional biopsy is usually performed when malignancy is suspected in order to obtain adequate tissue for histological diagnosis and biologic studies. The results of such studies are now incorporated into treatment protocols. Even in experienced hands, the histopathologic diagnosis of these tumors is difficult from fine needle aspiration[93].

Staging evaluation requires identification of all disease sites. Treatment protocols often stratify therapy based upon tumor histology, size and location of the primary tumor, involvement of other structures, presence or absence of metastatic sites and skip lesions. Bone sarcomas metastasize hematogenously primarily to lungs and later, to bone. As bone lacks lymphatics, only rarely has involvement of regional lymph nodes been reported and such a finding is associated with a poor prognosis[11]. Delineation of the primary bone tumor and any involvement of adjacent soft tissues, bony structures and vascular structures is important not only for disease staging, but for monitoring treatment response, planning surgery and, when appropriate, radiation therapy. The entire length of the involved bone must be imaged in order to accurately define its extent and to detect any skip lesions. Skip lesions represent embolic micrometastasis within marrow sinusoids of the same bone that are discontinuous from the primary tumor[60] (Figure 1). Transarticular skip metastases occur within the joint adjacent to the primary tumor. Skip lesions are usually seen with high-grade sarcomas and are prognostic of poor survival[11;60]. Preliminary report by Bruland et al suggests that at the time of primary diagnosis the presence of micrometastatic bone marrow disease determined by immunomagnetic isolation correlates with clinical stage and disease progression. However, such a technique is not currently in widespread clinical use[14].

Preliminary diagnosis is based upon radiographic findings coupled with the clinical history[9]. Contemporary imaging includes MR of the primary site of disease. The multiplanar capabilities of MR coupled with inherent tissue signal characteristics optimize tumor characterization, define involvement of adjacent soft tissues, delineate intramedullary extent of disease (Figure 2) and determine local or regional metastases. In some cases, MR may redirect clinical management by distinguishing between malignant (Figure 3) and non-malignant (Figure 4_) disease. Dynamic enhanced MR techniques obtained at the time of diagnosis provide baseline information for following tumor response to therapy[95-97] (Figure 5). Thus far, a prognostic role for such techniques based upon findings at the time of diagnosis has not been established[84].

Computed tomography (CT) of the chest is used for determination of pulmonary metastases. Unfortunately, even with the current quality of technology, the number of CT-determined pulmonary nodules correlates poorly with the number detected surgically, underestimating the number of lesions detected at surgery by 35%[63]. Rarely, can CT characteristics of these nodules be definitive for metastatic disease (Figure 6). Histologic diagnosis is frequently required as the presence of pulmonary metastases elevates disease staging in bone sarcomas and, thus, alters therapy. CT is helpful in these cases to direct surgical biopsy. Monitoring of

response of pulmonary metastases and identification of new lesions is routinely performed with chest CT.

Historically, 99mTc-MDP bone scans were utilized for delineating sites of distant bone metastases and for monitoring tumor response to therapy (Figure 2). However, 18F fluorodeoxyglucose (18F-FDG; a surrogate of glucose metabolism) PET/PET-CT is now being investigated to determine its role in staging and monitoring tumor response and in detecting recurrent and metastatic disease[19;27;34;39;42;79;105] (Figure 7). Preliminary results show 18F-FDG PET/PET-CT that may be a sensitive and promising modality for patients with bone sarcomas[12;30;34;39;67;70]. Investigation by Franzius et al also found that 18F-FDG PET had superior specificity, sensitivity and accuracy in detecting skeletal metastases compared with bone scintigraphy but when they analyzed these parameters by histologic diagnosis (I.e., osteosarcoma versus Ewing sarcoma), the superiority of 18F-FDG PET varied. Identification of bone metastases by 18F-FDG PET was superior to 99m-Tc-MDP bone scintigraphy in patients with Ewing sarcoma (sensitivity, specificity, accuracy of 18F-PET and bone scintigraphy of 1.00, 0.96, 0.97 versus 0.68, 0.87, 0.82, respectively). However, in cases of osteosarcoma, the investigators found bone scintigraphy to be superior to 18F-FDG PET having identified five metastatic bone lesions not demonstrated by 18F-FDG PET[39]. The ability of 18F-FDG PET/PET-CT to predict tumor grade (particularly with chondrosarcomas) is under investigation[19;70]. The information provided by 18F-FDG PET/PET-CT is particularly useful as a means of assessing metabolic treatment response coupled with anatomic and histologic tumor response.

IMAGING STRATEGY

Regardless of the type of bone sarcoma, imaging is critical to establishment of diagnosis, staging, surgical planning, assessment of therapeutic response, and off therapy monitoring.

Imaging at Diagnosis

Imaging performed at the time of diagnosis must define and characterize the primary bone lesion, its impact on adjacent soft tissues and determine the presence of metastatic disease. Radiographs provide the primary imaging investigation[29] followed by MR of the primary site of disease. MR must encompass the primary tumor site and the entire bone in which the tumor resides in order to identify any potential skip lesions[29;114]. Though rare (occurring in about 2% - 6.5% of cases of high-grade osteosarcoma and even fewer in Ewing sarcoma), skip lesions impart a significantly worse patient outcome[58;69;100] and necessitate modification of the surgical procedure[8;69] (Figure 1). Skip lesions are distinctly separate from the primary tumor and may occur in proximity to or distal from the primary tumor in the same bone or across the joint[8;69]. 99mTc-MDP bone scintigraphy has not been shown to be reliable in demonstrating skip metastases[8;69;100] or other multifocal bone lesions when compared to MR[82]. MR sequences typically comprise non-contrast T1, fat saturated T2, STIR, and post-contrast fat saturated T1 weighted sequences. These should be performed in at least two and preferably three planes with one longitudinal imaging sequence visualizing the entire bone[83;84;114]. Measurement of intramedullary tumor may be difficult in the presence of peritumoral edema. Non-contrast T1-weighted sequence[87], dynamic enhanced imaging[54;55] or combining T1-weighted with STIR sequence can be helpful[52] (Figures 1, 3

and 5) may aid in distinguishing tumor from surrounding edema. Most reports of skip lesions address their significance in osteosarcoma. However, the same considerations for imaging and surgical planning apply to the rarely reported cases of Ewing sarcoma in which skip lesions occur; the reported prognosis of such patients is dismal[59].

Accurate determination of tumor size is predictive of outcome in osteosarcoma. Absolute (but not relative) tumor volume is associated with a predictive value of overall survival (p=0.018) and event free survival (p=0.036) in pediatric nonmetastatic osteosarcoma of the extremity[62]. Measurement of intramedullary tumor extent is best demonstrated using a longitudinal T1-weighted non-contrast sequence of the involved bone[87] (Figures 2 and 3). Of particular importance in planning surgical procedures, is determination of tumor extension across the physis and into the epiphysis. Similarly, tumor size at the time of diagnosis of Ewing sarcoma is prognostically significant for patient outcome; volumetrically smaller tumors are associated with improved disease free survival[84].

Dynamic enhanced MR of the primary site of disease serves as an indicator of tumor perfusion, microcirculation and tumor interstitium. It serves as a surrogate variable for assessing drug delivery[67;95-97] but is not currently available for routine clinical use. This technique is an additional prognostic factor predictive of disease-free survival in patients receiving chemotherapy for osteosarcoma (p=0.035)[95;97]. A higher initial regional access of contrast was associated with greater disease-free survival[96]. With growing investigation of antiangiogenesis factors as therapeutic agents, the use and value of dynamic enhancement may become an imaging technique key to routine monitoring of chemotherapy perfusion of tumor and treatment response.

A prognostically significant role of 18F-FDG PET/PET-CT based upon the intensity of metabolic activity in the primary tumor at the time of diagnosis has been suggested. Franzius et al found that the maximum intensity of tumor to non-tumor uptake in osteosarcoma was statistically significantly correlated with overall (P<0.05) and event-free survival (P<0.005); high metabolic activity correlated with poor outcome[34]. Large prospective studies are needed to further define the role of 18F-FDG PET/PET-CT in the management of patients with osteosarcoma.

In addition to defining the primary tumor, metastatic disease must also be determined for complete staging. Chest CT is used for detection of pulmonary metastatic disease. Chest CT is considerably more sensitive than chest x-ray for detecting small pulmonary metastases[83]. PET/PET-CT shows strong promise for detecting distant metastases in cases of bone sarcoma (Figure 7), but is not without limitations. It has been shown to have up to 100% sensitivity in detecting distant metastatic sites but detection of pulmonary lesions smaller than 5mm in diameter typically fall below the resolution threshold of PET/PET-CT[35;66]. Pulmonary nodules between 5 and 9mm in size are often undetectable with PET-CT[35]. In addition, metabolic activity in benign lesions, in sites of infection and in normal structures particularly in pediatric patients, may complicate interpretation of FDG activity[7;35;37;103]. Thus, spiral CT remains the most sensitive modality currently available for detection of pulmonary metastases[35;37].

Detection of distant skeletal metastases has historically been performed with bone scintigraphy, preferably utilizing SPECT technique[83]. However, the use of F^{18} FDG-PET or PET-CT has grown over the past several years for staging bone sarcomas[6;29;83]. In comparison CT and MR, PET/PET-CT has been shown to be superior in detecting skeletal and soft tissue metastases[42;65;66;83;108]. PET/PET-CT may also be valuable in detecting skeletal metastases that demonstrate no abnormal activity by 99mTc-MDP bone scans[6].

Whole body MR techniques are currently under investigation for detection of skeletal metastases. Daldrup-Link et al studied 39 pediatric patients ranging in age from 2 to 19 years (osteosarcoma n=3, Ewing sarcoma n=20, other n=16). Using whole body spin echo MR, they found MR to have a higher sensitivity than 99m-Tc bone scans but lower sensitivity than F^{18} FDG-PET/PET-CT in detecting bone metastases[27].

Imaging During Therapy

Since most pediatric patients are treated on established therapeutic protocols, imaging timing is standardized by tumor type and treatment protocol. Additional imaging may be performed for clinical indications that arise outside of the protocol study design. Key factors to be addressed include change in size of the primary tumor, change in tumor imaging characteristics such as extent of necrosis, ossification, vascularity, response of metastases identified at the time of diagnosis and determination of new metastatic sites, identification of treatment sequelae. Establishment of new disease and/or progression of existing disease may prompt a change in planned therapy.

Static MR imaging provides the backbone for monitoring disease response to therapy of pediatric bone sarcomas. The clinical significance of a change in size depends upon the primary tumor type. Osteosarcoma decreases little in size during therapy[104] due to the dense osteoid. Historically, radiographic demonstration of increased ossification and improved demarcation of the soft tissue component indicated a favorable therapeutic response. However, neither radiographs nor CT are able to delineate viable residual from nonviable disease[104].

In contrast to osteosarcoma, therapeutic response of Ewing sarcomas is indicated by a decrease in tumor volume[104;106]. A reduction of less than 25% in tumor size and/or residual soft tissue mass correlated with a poor response[106]. Investigators found no correlation with signal intensity or its change during chemotherapy and histopathologic response[106].

A change in the extent and pattern of peritumoral edema has been explored as another imaging variable in assessing tumor response to therapy. MR-demonstration of decrease in peritumoral edema has been suggested as a favorable sign of chemotherapeutic response in cases of osteosarcoma[33;53;55;89] and Ewing sarcoma[106], alike.

Dynamic enhanced MR sequences demonstrating and quantifying the degree of tumor necrosis as an indicator of biologic response is also now possible[28;95-97] (Figure 5). The slope of linear regression of the regional access of contrast is predictive of disease free survival. After preoperative chemotherapy, Reddick et al showed that a lower regional access of contrast to tumor was predictive of better outcome in primary osteosarcoma[96].

Similar findings have been reported in series of both osteosarcoma and Ewing sarcoma[28]. MR-determined per cent of tumoral necrosis in both osteosarcoma and Ewing sarcoma correlates well with histopathologic determination of tumor necrosis[28;106].

Also undergoing assessment of its role in determining biologic response to therapy in bone sarcomas is PET/PET-CT[38;67]. The greatest experience with this technique in bone sarcomas is using 18F-FDG. A favorable response to therapy is indicated by a decrease in metabolic activity in tumor sites which correlates with reduced tumor cell viability[12;30;38;67]. Brenner et al found that patients at increased risk for local disease recurrence or development of metastatic disease could be identified by combining the pre-treatment SUV and histopathologic tumor grade[12]. Other investigators found that a reduction in tumor to non-tumor ratios of 18F-FDG PET exceeding 30% was associated with good response to chemotherapy and that 18F-FDG PET was superior to 99m-Tc-MDP bone scans in determining histologic response to therapy in pediatric cases[38]. Similarly, Hawkins et al found the initial response to therapy may be predictive of outcome as measured by a decrease in SUV after induction chemotherapy in Ewings sarcoma[50].These investigators failed to find the same prognostic significance in cases of osteosarcoma[49]. More recently, the sensitivity, specificity and accuracy of PET-CT was found to be superior to PET alone in staging and following patients with Ewings sarcoma[42]. The long-term prognostic value of such information has yet to be fully established.

The roles for disease staging, tumor grading and assessment of therapeutic response of additional radiopharmaceutical agents such as 11C-methionine[43;67] and 3'-deoxy – 3' – F-18- fluorothymidine (18F-FLT) are currently under investigation[2;15;21;30;67;73]. Preliminary work by Buck et al found that 18F-FLT identified all malignant bone and soft tissue tumors and effectively discriminated between low and high-grade tumors when a maximum SUV of 2.0 was used as the cut-off value[15]. As discussed, non-invasive assessment and monitoring of disease is optimized by merging biological tumor activity with anatomic characteristics. Under development is merging of biologic information of PET with the refined anatomic and dynamic imaging of MR resulting in PETMR[112;113;116] (Figure 8).

Imaging during Follow-up

Despite advances in staging and treatment of bone sarcomas, approximately 30% of patients with osteosarcoma will develop disease relapse, most often involving the lungs[32;51]. Local relapse in patients with non-metastatic extremity osteosarcoma is independently associated with tumor response to therapy, inadequacy of surgical margins[4] tumor volume, age at diagnosis, and histologic subtype[31]. Most instances of disease relapse develops within 2 to 3 years of diagnosis but e occurring beyond 4 years occurs [31;105;110].

Of patients treated for Ewing sarcoma, 30-40% can be expected to develop local and/or distant recurrent disease typically occurring between 2 and 10 years after diagnosis. However, rare cases of delayed recurrence at 16 and 19 years after diagnosis have been reported[48]. More than half of these patients will have pulmonary or skeletal disease[24]. The recent report from the Childhood Cancer Survivor Study found that survivors of pediatric Ewings sarcoma had the highest 20-year cumulative incidence of recurrent disease amongst

eight pediatric tumor categories, estimated at 13% (95% confidence interval [CI]=9.4 to 16.5)[110]. Local recurrent disease from chondrosarcoma is not uncommon but distant metastases are rare and may develop years after initial treatment[75]. Thus, patients with bone sarcomas are monitored for at least 5 years after diagnosis[75]. Recent guidelines from the Children's Oncology Group Bone Tumor Committee suggest 10 years of follow-up for monitoring primary and metastatic disease[83].

Local disease recurrence is often suspected clinically because of the patient returning with pain or development of a mass. Radiographs remain the front-line imaging study the primary skeletal disease site and of those suspected of metastatic involvement providing important information regarding prosthesis integrity in patients who underwent limb-sparing procedures[23]. Further, radiographs are useful for demonstrating processes that may symptomatically mimic disease recurrence such as fractures. Imaging with MR, CT, PET/PET-CT and even 99mTc-MDP bone scans provide information important for disease characterization and detection of distant metastases. Asymmetric weight-bearing related to prior surgery, radiation therapy or the use of a prosthesis make interpretation of PET/PET-CT and 99mTc-MDP bone scans more difficult[75]. Sensitivity, specificity and accuracy of PET detection of bone sarcoma recurrence are reported to be 0.96, 0.81 and 0.90, respectively, and exceed those of conventional imaging techniques (1.00, 0.56 and 0,82, respectively)[36].

Interpretation of the imaging findings may be complicated by prior treatment. The usefulness of CT and MR in detecting new or assessing known recurrence may be compromised in the presence of a metallic prosthesis that creates significant artifact. Metallic artifact can be decreased in MR by using T(1)-weighted turbo spin echo and turbo short tau inversion recovery (STIR) with high bandwidth and short echo times[107]. Chest CT is performed serially for several years after diagnosis. The frequency varies somewhat by treatment protocol and tumor type, are typically performed every 4 to 6 months for several years followed subsequently by less frequent monitoring[75]. CT is unable to distinguish between benign and metastatic pulmonary nodules in children with known malignant solid tumors[81]. A similar dilemma occurs in patients who have previously undergone a thoracotomy (Figure 9). In one series of pediatric osteosarcoma patients, pulmonary nodules recurred in 32 of 35 patients with a history of prior thoracotomy. The only finding consistently found to indicate recurrent metastatic disease was progression of pleural thickening. The authors also found that the development of a pulmonary nodule in the lung contralateral to the prior thoracotomy was most often malignant[80].

SUMMARY

Diagnostic imaging is a critical component to the multidisciplinary management of pediatric bone sarcomas. From diagnosis through post-therapy monitoring, imaging identifies disease, monitors tumor response to therapy and guides follow-up intervention. The evolution of imaging techniques that combine biologic and anatomic information is ongoing and should further augment pediatric oncologic care.

ACKNOWLEDGEMENTS

I thank Dr. Stephen F. Miller for critical review of the manuscript and Sandra Gaither for manuscript preparation.

This work was supported in part by grants P30 CA-21765 and P01 CA-20180 from the National Institutes of Health, a Center of Excellence grant from the State of Tennessee, and the American Lebanese Syrian Associated Charities (ALSAC).

Reference List

1. Ahmed AR, Tan TS, Unni KK, Collins MS, Wenger DE, Sim FH. Secondary chondrosarcoma in osteochondroma: report of 107 patients. Clin Orthop Relat Res. 2003; (411):193–206. [PubMed: 12782876]
2. Arvanitis C, Bendapudi PK, Tseng JR, Gambhir SS, Felsher DW. (18)F and (18)FDG PET imaging of osteosarcoma to non-invasively monitor in situ changes in cellular proliferation and bone differentiation upon MYC inactivation. Cancer Biol Ther. 2008; 7(12):1947–1951. [PubMed: 18981708]
3. Bacci G, Ferrari S, Bertoni F, Rimondini S, Longhi A, Bacchini P, et al. Prognostic factors in nonmetastatic Ewing's sarcoma of bone treated with adjuvant chemotherapy: analysis of 359 patients at the Istituto Ortopedico Rizzoli. J Clin Oncol. 2000; 18(1):4–11. [PubMed: 10623687]
4. Bacci G, Forni C, Longhi A, Ferrari S, Mercuri M, Bertoni F, et al. Local recurrence and local control of non-metastatic osteosarcoma of the extremities: a 27-year experience in a single institution. J Surg Oncol. 2007; 96(2):118–123. [PubMed: 17577221]
5. Bacci G, Longhi A, Ferrari S, Mercuri M, Versari M, Bertoni F. Prognostic factors in non-metastatic Ewing's sarcoma tumor of bone: an analysis of 579 patients treated at a single institution with adjuvant or neoadjuvant chemotherapy between 1972 and 1998. Acta Oncol. 2006; 45(4):469–475. [PubMed: 16760184]
6. Benz MR, Tchekmedyian N, Eilber FC, Federman N, Czernin J, Tap WD. Utilization of positron emission tomography in the management of patients with sarcoma. Curr Opin Oncol. 2009; 21(4): 345–351. [PubMed: 19412096]
7. Bestic JM, Peterson JJ, Bancroft LW. Pediatric FDG PET/CT: Physiologic uptake, normal variants, and benign conditions [corrected]. Radiographics. 2009; 29(5):1487–1500. [PubMed: 19755607]
8. Bhagia SM, Grimer RJ, Davies AM, Mangham DC. Scintigraphically negative skip metastasis in osteosarcoma. Eur Radiol. 1997; 7(9):1446–1448. [PubMed: 9369512]
9. Bielack SS, Carrle D. State-of-the-art approach in selective curable tumors: bone sarcoma. Ann Oncol. 2008; 19(Suppl 7):vii155–vii160. [PubMed: 18790938]
10. Bovee JV. Multiple osteochondromas. Orphanet J Rare Dis. 2008; 33
11. Brennan, MF.; Singer, S.; Maki, RG.; O'Sullivan, B. Soft Tissue Sarcoma.. In: DeVita, VT., Jr.; Lawrence, TS.; Rosenberg, SA., editors. Devita, Hellman & Rosenberg's Cancer: Principles & Practice of Oncology. 8th edition. Lippincott Williams & Wilkins; Philadelphia, PA: 2010.
12. Brenner W, Conrad EU, Eary JF. FDG PET imaging for grading and prediction of outcome in chondrosarcoma patients. Eur J Nucl Med Mol Imaging. 2004; 31(2):189–195. [PubMed: 15129700]
13. Brisse HJ. Staging of common paediatric tumours. Pediatr Radiol. 2009; 39(Suppl 3):482–490. [PubMed: 19440769]
14. Bruland OS, Hoifodt H, Hall KS, Smeland S, Fodstad O. Bone Marrow Micrometastases Studied by an Immunomagnetic Isolation Procedure in Extremity Localized Non-metastatic Osteosarcoma Patients. Cancer Treat Res. 2010; 152:509–515. [PubMed: 20213412]
15. Buck AK, Herrmann K, Buschenfelde CM, Juweid ME, Bischoff M, Glatting G, et al. Imaging bone and soft tissue tumors with the proliferation marker [18F]fluorodeoxythymidine. Clin Cancer Res. 2008; 14(10):2970–2977. [PubMed: 18445694]
16. Caudill JS, Arndt CA. Diagnosis and management of bone malignancy in adolescence. Adolesc Med State Art Rev. 2007; 18(1):62–78, ix. [PubMed: 18605391]

17. Cesari M, Bertoni F, Bacchini P, Mercuri M, Palmerini E, Ferrari S. Mesenchymal chondrosarcoma. An analysis of patients treated at a single institution. Tumori. 2007; 93(5):423–427. [PubMed: 18038872]
18. Chaabane S, Bouaziz MC, Drissi C, Abid L, Ladeb MF. Periosteal chondrosarcoma. AJR Am J Roentgenol. 2009; 192(1):W1–W6. [PubMed: 19098166]
19. Charest M, Hickeson M, Lisbona R, Novales-Diaz JA, Derbekyan V, Turcotte RE. FDG PET/CT imaging in primary osseous and soft tissue sarcomas: a retrospective review of 212 cases. Eur J Nucl Med Mol Imaging. 2009
20. Chow WA. Update on chondrosarcomas. Curr Opin Oncol. 2007; 19(4):371–376. [PubMed: 17545802]
21. Cobben DC, Elsinga PH, Suurmeijer AJ, Vaalburg W, Maas B, Jager PL, et al. Detection and grading of soft tissue sarcomas of the extremities with (18)F-3'-fluoro-3'-deoxy-L-thymidine. Clin Cancer Res. 2004; 10(5):1685–1690. [PubMed: 15014020]
22. Collins MS, Koyama T, Swee RG, Inwards CY. Clear cell chondrosarcoma: radiographic, computed tomographic, and magnetic resonance findings in 34 patients with pathologic correlation. Skeletal Radiol. 2003; 32(12):687–694. [PubMed: 14530882]
23. Costelloe CM, Kumar R, Yasko AW, Murphy WA Jr. Stafford RJ, Lewis VO, et al. Imaging characteristics of locally recurrent tumors of bone. AJR Am J Roentgenol. 2007; 188(3):855–863. [PubMed: 17312079]
24. Cotterill SJ, Ahrens S, Paulussen M, Jurgens HF, Voute PA, Gadner H, et al. Prognostic factors in Ewing's tumor of bone: analysis of 975 patients from the European Intergroup Cooperative Ewing's Sarcoma Study Group. J Clin Oncol. 2000; 18(17):3108–3114. [PubMed: 10963639]
25. Damron TA, Ward WG, Stewart A. Osteosarcoma, chondrosarcoma, and Ewing's sarcoma: National Cancer Data Base Report. Clin Orthop Relat Res. 2007; 459:40–47. [PubMed: 17414166]
26. Dantonello TM, Int-Veen C, Leuschner I, Schuck A, Furtwaengler R, Claviez A, et al. Mesenchymal chondrosarcoma of soft tissues and bone in children, adolescents, and young adults: experiences of the CWS and COSS study groups. Cancer. 2008; 112(11):2424–2431. [PubMed: 18438777]
27. drup-Link HE, Franzius C, Link TM, Laukamp D, Sciuk J, Jurgens H, et al. Whole-body MR imaging for detection of bone metastases in children and young adults: comparison with skeletal scintigraphy and FDG PET. AJR Am J Roentgenol. 2001; 177(1):229–236. [PubMed: 11418435]
28. Dyke JP, Panicek DM, Healey JH, Meyers PA, Huvos AG, Schwartz LH, et al. Osteogenic and Ewing sarcomas: estimation of necrotic fraction during induction chemotherapy with dynamic contrast-enhanced MR imaging. Radiology. 2003; 228(1):271–278. [PubMed: 12832588]
29. Federman N, Bernthal N, Eilber FC, Tap WD. The multidisciplinary management of osteosarcoma. Curr Treat Options Oncol. 2009; 10(1-2):82–93. [PubMed: 19238553]
30. Feldman F, Van HR, Saxena C, Parisien M. 18FDG-PET applications for cartilage neoplasms. Skeletal Radiol. 2005; 34(7):367–374. [PubMed: 15937711]
31. Ferrari S, Bertoni F, Mercuri M, Picci P, Giacomini S, Longhi A, et al. Predictive factors of disease-free survival for non-metastatic osteosarcoma of the extremity: an analysis of 300 patients treated at the Rizzoli Institute. Ann Oncol. 2001; 12(8):1145–1150. [PubMed: 11583198]
32. Ferrari S, Briccoli A, Mercuri M, Bertoni F, Picci P, Tienghi A, et al. Postrelapse survival in osteosarcoma of the extremities: prognostic factors for long-term survival. J Clin Oncol. 2003; 21(4):710–715. [PubMed: 12586810]
33. Fletcher BD. Response of osteosarcoma and Ewing sarcoma to chemotherapy: imaging evaluation. AJR Am J Roentgenol. 1991; 157(4):825–833. [PubMed: 1892044]
34. Franzius C, Bielack S, Flege S, Sciuk J, Jurgens H, Schober O. Prognostic significance of (18)F-FDG and (99m)Tc-methylene diphosphonate uptake in primary osteosarcoma. J Nucl Med. 2002; 43(8):1012–1017. [PubMed: 12163625]
35. Franzius C, drup-Link HE, Sciuk J, Rummeny EJ, Bielack S, Jurgens H, et al. FDG-PET for detection of pulmonary metastases from malignant primary bone tumors: comparison with spiral CT. Ann Oncol. 2001; 12(4):479–486. [PubMed: 11398879]

36. Franzius C, drup-Link HE, Wagner-Bohn A, Sciuk J, Heindel WL, Jurgens H, et al. FDG-PET for detection of recurrences from malignant primary bone tumors: comparison with conventional imaging. Ann Oncol. 2002; 13(1):157–160. [PubMed: 11863097]
37. Franzius C, Juergens KU. PET/CT in paediatric oncology: indications and pitfalls. Pediatr Radiol. 2009; 39(Suppl 3):446–449. [PubMed: 19440764]
38. Franzius C, Sciuk J, Brinkschmidt C, Jurgens H, Schober O. Evaluation of chemotherapy response in primary bone tumors with F-18 FDG positron emission tomography compared with histologically assessed tumor necrosis. Clin Nucl Med. 2000; 25(11):874–881. [PubMed: 11079583]
39. Franzius C, Sciuk J, drup-Link HE, Jurgens H, Schober O. FDG-PET for detection of osseous metastases from malignant primary bone tumours: comparison with bone scintigraphy. Eur J Nucl Med. 2000; 27(9):1305–1311. [PubMed: 11007511]
40. Geirnaerdt MJ, Hogendoorn PC, Bloem JL, Taminiau AH, van der Woude HJ. Cartilaginous tumors: fast contrast-enhanced MR imaging. Radiology. 2000; 214(2):539–546. [PubMed: 10671608]
41. Gelderblom H, Hogendoorn PC, Dijkstra SD, van Rijswijk CS, Krol AD, Taminiau AH, et al. The clinical approach towards chondrosarcoma. Oncologist. 2008; 13(3):320–329. [PubMed: 18378543]
42. Gerth HU, Juergens KU, Dirksen U, Gerss J, Schober O, Franzius C. Significant benefit of multimodal imaging: PET/CT compared with PET alone in staging and follow-up of patients with Ewing tumors. J Nucl Med. 2007; 48(12):1932–1939. [PubMed: 18006618]
43. Ghigi G, Micera R, Maffione AM, Castellucci P, Cammelli S, Ammendolia I, et al. 11C-methionine vs. 18F-FDG PET in soft tissue sarcoma patients treated with neoadjuvant therapy: preliminary results. In Vivo. 2009; 23(1):105–110. [PubMed: 19368133]
44. Giuffrida AY, Burgueno JE, Koniaris LG, Gutierrez JC, Duncan R, Scully SP. Chondrosarcoma in the United States (1973 to 2003): an analysis of 2890 cases from the SEER database. J Bone Joint Surg Am. 2009; 91(5):1063–1072. [PubMed: 19411454]
45. Grier HE, Krailo MD, Tarbell NJ, Link MP, Fryer CJ, Pritchard DJ, et al. Addition of ifosfamide and etoposide to standard chemotherapy for Ewing's sarcoma and primitive neuroectodermal tumor of bone. N Engl J Med. 2003; 348(8):694–701. [PubMed: 12594313]
46. Hall EJ. Radiation biology for pediatric radiologists. Pediatr Radiol. 2009; 39(Suppl 1):S57–S64. [PubMed: 19083223]
47. Hallor KH, Staaf J, Bovee JV, Hogendoorn PC, Cleton-Jansen AM, Knuutila S, et al. Genomic profiling of chondrosarcoma: chromosomal patterns in central and peripheral tumors. Clin Cancer Res. 2009; 15(8):2685–2694. [PubMed: 19336518]
48. Hanna SA, David LA, Gikas PD, Tindall AJ, Cannon SR, Briggs TW. Very late local recurrence of Ewing's sarcoma--can you ever say ‘cured’? A report of two cases and literature review. Ann R Coll Surg Engl. 2008; 90(7):W12–W15. [PubMed: 18831863]
49. Hawkins DS, Conrad EU III, Butrynski JE, Schuetze SM, Eary JF. [F-18]-fluorodeoxy-D-glucose-positron emission tomography response is associated with outcome for extremity osteosarcoma in children and young adults. Cancer. 2009; 115(15):3519–3525. [PubMed: 19517457]
50. Hawkins DS, Schuetze SM, Butrynski JE, Rajendran JG, Vernon CB, Conrad EU III, et al. [18F]Fluorodeoxyglucose positron emission tomography predicts outcome for Ewing sarcoma family of tumors. J Clin Oncol. 2005; 23(34):8828–8834. [PubMed: 16314643]
51. Heare T, Hensley MA, Dell'Orfano S. Bone tumors: osteosarcoma and Ewing's sarcoma. Curr Opin Pediatr. 2009; 21(3):365–372. [PubMed: 19421061]
52. Hoffer FA, Nikanorov AY, Reddick WE, Bodner SM, Xiong X, Jones-Wallace D, et al. Accuracy of MR imaging for detecting epiphyseal extension of osteosarcoma. Pediatr Radiol. 2000; 30(5): 289–298. [PubMed: 10836589]
53. Holscher HC, Bloem JL, Vanel D, Hermans J, Nooy MA, Taminiau AH, et al. Osteosarcoma: chemotherapy-induced changes at MR imaging. Radiology. 1992; 182(3):839–844. [PubMed: 1535905]

54. Iwasawa T, Tanaka Y, Aida N, Okuzumi S, Nishihira H, Nishimura G. Microscopic intraosseous extension of osteosarcoma: assessment on dynamic contrast-enhanced MRI. Skeletal Radiol. 1997; 26(4):214–221. [PubMed: 9151369]
55. James SL, Panicek DM, Davies AM. Bone marrow oedema associated with benign and malignant bone tumours. Eur J Radiol. 2008; 67(1):11–21. [PubMed: 18358660]
56. Janzen L, Logan PM, O'Connell JX, Connell DG, Munk PL. Intramedullary chondroid tumors of bone: correlation of abnormal peritumoral marrow and soft-tissue MRI signal with tumor type. Skeletal Radiol. 1997; 26(2):100–106. [PubMed: 9060101]
57. Jawad MU, Cheung MC, Min ES, Schneiderbauer MM, Koniaris LG, Scully SP. Ewing sarcoma demonstrates racial disparities in incidence-related and sex-related differences in outcome: an analysis of 1631 cases from the SEER database, 1973-2005. Cancer. 2009; 115(15):3526–3536. [PubMed: 19548262]
58. Jeon DG, Kim MS, Cho WH, Song WS, Lee SY. Clinical outcome of osteosarcoma with primary total femoral resection. Clin Orthop Relat Res. 2007; 457:176–182. [PubMed: 17075378]
59. Jiya TU, Wuisman PI. Long-term follow-up of 15 patients with non-metastatic Ewing's sarcoma and a skip lesion. Acta Orthop. 2005; 76(6):899–903. [PubMed: 16470449]
60. Kager L, Zoubek A, Kastner U, Kempf-Bielack B, Potratz J, Kotz R, et al. Skip metastases in osteosarcoma: experience of the Cooperative Osteosarcoma Study Group. J Clin Oncol. 2006; 24(10):1535–1541. [PubMed: 16575004]
61. Kaste SC, Fuller CE, Saharia A, Neel MD, Rao BN, Daw NC. Pediatric surface osteosarcoma: clinical, pathologic, and radiologic features. Pediatr Blood Cancer. 2006; 47(2):152–162. [PubMed: 16123997]
62. Kaste SC, Liu T, Billups CA, Daw NC, Pratt CB, Meyer WH. Tumor size as a predictor of outcome in pediatric non-metastatic osteosarcoma of the extremity. Pediatr Blood Cancer. 2004; 43(7):723–728. [PubMed: 15390310]
63. Kayton ML, Huvos AG, Casher J, Abramson SJ, Rosen NS, Wexler LH, et al. Computed tomographic scan of the chest underestimates the number of metastatic lesions in osteosarcoma. J Pediatr Surg. 2006; 41(1):200–206. [PubMed: 16410133]
64. King MA, Kanal KM, Relyea-Chew A, Bittles M, Vavilala MS, Hollingworth W. Radiation exposure from pediatric head CT: a bi-institutional study. Pediatr Radiol. 2009; 39(10):1059–1065. [PubMed: 19554322]
65. Kleis M, drup-Link H, Matthay K, Goldsby R, Lu Y, Schuster T, et al. Diagnostic value of PET/CT for the staging and restaging of pediatric tumors. Eur J Nucl Med Mol Imaging. 2009; 36(1):23–36. [PubMed: 18719909]
66. Kumar R, Chauhan A, Vellimana AK, Chawla M. Role of PET/PET-CT in the management of sarcomas. Expert Rev Anticancer Ther. 2006; 6(8):1241–1250. [PubMed: 16925490]
67. Landa J, Schwartz LH. Contemporary imaging in sarcoma. Oncologist. 2009; 14(10):1021–1038. [PubMed: 19789392]
68. Leavey PJ, Collier AB. Ewing sarcoma: prognostic criteria, outcomes and future treatment. Expert Rev Anticancer Ther. 2008; 8(4):617–624. [PubMed: 18402528]
69. Leavey PJ, Day MD, Booth T, Maale G. Skip metastasis in osteosarcoma. J Pediatr Hematol Oncol. 2003; 25(10):806–808. [PubMed: 14528105]
70. Lee FY, Yu J, Chang SS, Fawwaz R, Parisien MV. Diagnostic value and limitations of fluorine-18 fluorodeoxyglucose positron emission tomography for cartilaginous tumors of bone. J Bone Joint Surg Am. 2004; 86-A(12):2677–2685. [PubMed: 15590853]
71. Lee JA, Kim MS, Kim DH, Lim JS, Yoo JY, Koh JS, et al. Relative tumor burden predicts metastasis-free survival in pediatric osteosarcoma. Pediatr Blood Cancer. 2008; 50(2):195–200. [PubMed: 18061933]
72. Lewis VO. What's new in musculoskeletal oncology. J Bone Joint Surg Am. 2009; 91(6):1546–1556. [PubMed: 19487537]
73. Leyton J, Latigo JR, Perumal M, Dhaliwal H, He Q, Aboagye EO. Early detection of tumor response to chemotherapy by 3'-deoxy-3'-[18F]fluorothymidine positron emission tomography: the effect of cisplatin on a fibrosarcoma tumor model in vivo. Cancer Res. 2005; 65(10):4202–4210. [PubMed: 15899811]

74. Lin PP, Jaffe N, Herzog CE, Costelloe CM, Deavers MT, Kelly JS, et al. Chemotherapy response is an important predictor of local recurrence in Ewing sarcoma. Cancer. 2007; 109(3):603–611. [PubMed: 17177205]
75. Link, MP.; Gebhardt, MC.; Mark, PC. Osteosarcoma.. In: Pizzo, PA.; Poplack, DG., editors. Principles & Practice of Pediatric Oncology. 5th edition. Lippincott Williams & Wilkins; Philadelphia: 2010.
76. Littrell LA, Wenger DE, Wold LE, Bertoni F, Unni KK, White LM, et al. Radiographic, CT, and MR imaging features of dedifferentiated chondrosarcomas: a retrospective review of 174 de novo cases. Radiographics. 2004; 24(5):1397–1409. [PubMed: 15371616]
77. Longhi A, Errani C, De PM, Mercuri M, Bacci G. Primary bone osteosarcoma in the pediatric age: state of the art. Cancer Treat Rev. 2006; 32(6):423–436. [PubMed: 16860938]
78. Ludwig JA. Ewing sarcoma: historical perspectives, current state-of-the-art, and opportunities for targeted therapy in the future. Curr Opin Oncol. 2008; 20(4):412–418. [PubMed: 18525337]
79. Mar WA, Taljanovic MS, Bagatell R, Graham AR, Speer DP, Hunter TB, et al. Update on imaging and treatment of Ewing sarcoma family tumors: what the radiologist needs to know. J Comput Assist Tomogr. 2008; 32(1):108–118. [PubMed: 18303298]
80. McCarville MB, Kaste SC, Cain AM, Goloubeva O, Rao BN, Pratt CB. Prognostic factors and imaging patterns of recurrent pulmonary nodules after thoracotomy in children with osteosarcoma. Cancer. 2001; 91(6):1170–1176. [PubMed: 11267963]
81. McCarville MB, Lederman HM, Santana VM, Daw NC, Shochat SJ, Li CS, et al. Distinguishing benign from malignant pulmonary nodules with helical chest CT in children with malignant solid tumors. Radiology. 2006; 239(2):514–520. [PubMed: 16641356]
82. Mentzel HJ, Kentouche K, Sauner D, Fleischmann C, Vogt S, Gottschild D, et al. Comparison of whole-body STIR-MRI and 99mTc-methylene-diphosphonate scintigraphy in children with suspected multifocal bone lesions. Eur Radiol. 2004; 14(12):2297–2302. [PubMed: 15243716]
83. Meyer JS, Nadel HR, Marina N, Womer RB, Brown KL, Eary JF, et al. Imaging guidelines for children with Ewing sarcoma and osteosarcoma: a report from the Children's Oncology Group Bone Tumor Committee. Pediatr Blood Cancer. 2008; 51(2):163–170. [PubMed: 18454470]
84. Miller SL, Hoffer FA, Reddick WE, Wu S, Glass JO, Gronemeyer SA, et al. Tumor volume or dynamic contrast-enhanced MRI for prediction of clinical outcome of Ewing sarcoma family of tumors. Pediatr Radiol. 2001; 31(7):518–523. [PubMed: 11486808]
85. Mirabello L, Troisi RJ, Savage SA. Osteosarcoma incidence and survival rates from 1973 to 2004: data from the Surveillance, Epidemiology, and End Results Program. Cancer. 2009; 115(7):1531–1543. [PubMed: 19197972]
86. Murphey MD, Walker EA, Wilson AJ, Kransdorf MJ, Temple HT, Gannon FH. From the archives of the AFIP: imaging of primary chondrosarcoma: radiologic-pathologic correlation. Radiographics. 2003; 23(5):1245–1278. [PubMed: 12975513]
87. Onikul E, Fletcher BD, Parham DM, Chen G. Accuracy of MR imaging for estimating intraosseous extent of osteosarcoma. AJR Am J Roentgenol. 1996; 167(5):1211–1215. [PubMed: 8911182]
88. Pahade J, Sekhar A, Shetty SK. Imaging of malignant skeletal tumors. Cancer Treat Res. 2008; 143:367–422. [PubMed: 18619226]
89. Pan G, Raymond AK, Carrasco CH, Wallace S, Kim EE, Shirkhoda A, et al. Osteosarcoma: MR imaging after preoperative chemotherapy. Radiology. 1990; 174(2):517–526. [PubMed: 2296660]
90. Papachristou DJ, Gkretsi V, Rao UN, Papachristou GI, Papaefthymiou OA, Basdra EK, et al. Expression of integrin-linked kinase and its binding partners in chondrosarcoma: association with prognostic significance. Eur J Cancer. 2008; 44(16):2518–2525. [PubMed: 18722108]
91. Papachristou DJ, Papavassiliou AG. Osteosarcoma and chondrosarcoma: new signaling pathways as targets for novel therapeutic interventions. Int J Biochem Cell Biol. 2007; 39(5):857–862. [PubMed: 17241811]
92. Paterson A, Frush DP. Dose reduction in paediatric MDCT: general principles. Clin Radiol. 2007; 62(6):507–517. [PubMed: 17467387]
93. Pohar-Marinsek Z. Difficulties in diagnosing small round cell tumours of childhood from fine needle aspiration cytology samples. Cytopathology. 2008; 19(2):67–79. [PubMed: 18352861]

94. Puri A, Shah M, Agarwal MG, Jambhekar NA, Basappa P. Chondrosarcoma of bone: does the size of the tumor, the presence of a pathologic fracture, or prior intervention have an impact on local control and survival? J Cancer Res Ther. 2009; 5(1):14–19. [PubMed: 19293483]

95. Reddick WE, Bhargava R, Taylor JS, Meyer WH, Fletcher BD. Dynamic contrast-enhanced MR imaging evaluation of osteosarcoma response to neoadjuvant chemotherapy. J Magn Reson Imaging. 1995; 5(6):689–694. [PubMed: 8748487]

96. Reddick WE, Taylor JS, Fletcher BD. Dynamic MR imaging (DEMRI) of microcirculation in bone sarcoma. J Magn Reson Imaging. 1999; 10(3):277–285. [PubMed: 10508287]

97. Reddick WE, Wang S, Xiong X, Glass JO, Wu S, Kaste SC, et al. Dynamic magnetic resonance imaging of regional contrast access as an additional prognostic factor in pediatric osteosarcoma. Cancer. 2001; 91(12):2230–2237. [PubMed: 11413510]

98. Riedel RF, Larrier N, Dodd L, Kirsch D, Martinez S, Brigman BE. The clinical management of chondrosarcoma. Curr Treat Options Oncol. 2009; 10(1-2):94–106. [PubMed: 19238552]

99. Ryzewicz M, Manaster BJ, Naar E, Lindeque B. Low-grade cartilage tumors: diagnosis and treatment. Orthopedics. 2007; 30(1):35–46. [PubMed: 17260660]

100. Sajadi KR, Heck RK, Neel MD, Rao BN, Daw N, Rodriguez-Galindo C, et al. The incidence and prognosis of osteosarcoma skip metastases. Clin Orthop Relat Res. 2004; (426):92–96. [PubMed: 15346057]

101. Schrage YM, Machado I, Meijer D, Briaire-de B I, van den Akker BE, Taminiau AH, et al. COX-2 expression in chondrosarcoma: a role for celecoxib treatment? Eur J Cancer. 2010; 46(3): 616–624. [PubMed: 20004565]

102. Semelka RC, Armao DM, Elias J Jr. Huda W. Imaging strategies to reduce the risk of radiation in CT studies, including selective substitution with MRI. J Magn Reson Imaging. 2007; 25(5):900–909. [PubMed: 17457809]

103. Shammas A, Lim R, Charron M. Pediatric FDG PET/CT: physiologic uptake, normal variants, and benign conditions. Radiographics. 2009; 29(5):1467–1486. [PubMed: 19755606]

104. Shapeero LG, Vanel D. Imaging evaluation of the response of high-grade osteosarcoma and Ewing sarcoma to chemotherapy with emphasis on dynamic contrast-enhanced magnetic resonance imaging. Semin Musculoskelet Radiol. 2000; 4(1):137–146. [PubMed: 11061698]

105. Stauss J, Franzius C, Pfluger T, Juergens KU, Biassoni L, Begent J, et al. Guidelines for 18F-FDG PET and PET-CT imaging in paediatric oncology. Eur J Nucl Med Mol Imaging. 2008; 35(8):1581–1588. [PubMed: 18536914]

106. van der Woude HJ, Bloem JL, Holscher HC, Nooy MA, Taminiau AH, Hermans J, et al. Monitoring the effect of chemotherapy in Ewing's sarcoma of bone with MR imaging. Skeletal Radiol. 1994; 23(7):493–500. [PubMed: 7824974]

107. Viano AM, Gronemeyer SA, Haliloglu M, Hoffer FA. Improved MR imaging for patients with metallic implants. Magn Reson Imaging. 2000; 18(3):287–295. [PubMed: 10745138]

108. Volker T, Denecke T, Steffen I, Misch D, Schonberger S, Plotkin M, et al. Positron emission tomography for staging of pediatric sarcoma patients: results of a prospective multicenter trial. J Clin Oncol. 2007; 25(34):5435–5441. [PubMed: 18048826]

109. Voss SD, Reaman GH, Kaste SC, Slovis TL. The ALARA concept in pediatric oncology. Pediatr Radiol. 2009; 39(11):1142–1146. [PubMed: 19789861]

110. Wasilewski-Masker K, Liu Q, Yasui Y, Leisenring W, Meacham LR, Hammond S, et al. Late recurrence in pediatric cancer: a report from the Childhood Cancer Survivor Study. J Natl Cancer Inst. 2009; 101(24):1709–1720. [PubMed: 19966206]

111. Weber KL. What's new in musculoskeletal oncology. J Bone Joint Surg Am. 2005; 87(6):1400–1410. [PubMed: 15930555]

112. Wehrl HF, Judenhofer MS, Wiehr S, Pichler BJ. Pre-clinical PET/MR: technological advances and new perspectives in biomedical research. Eur J Nucl Med Mol Imaging. 2009; 36(Suppl 1):S56–S68. [PubMed: 19194703]

113. Wehrl HF, Sauter AW, Judenhofer MS, Pichler BJ. Combined PET/MR imaging--technology and applications. Technol Cancer Res Treat. 2010; 9(1):5–20. [PubMed: 20082526]

114. Wootton-Gorges SL. MR imaging of primary bone tumors and tumor-like conditions in children. Magn Reson Imaging Clin N Am. 2009; 17(3):469–87, vi. [PubMed: 19524197]

115. Wunder JS, Nielsen TO, Maki RG, O'Sullivan B, Alman BA. Opportunities for improving the therapeutic ratio for patients with sarcoma. Lancet Oncol. 2007; 8(6):513–524. [PubMed: 17540303]

116. Zaidi H, Montandon ML, Alavi A. The clinical role of fusion imaging using PET, CT, and MR imaging. Magn Reson Imaging Clin N Am. 2010; 18(1):133–149. [PubMed: 19962098]

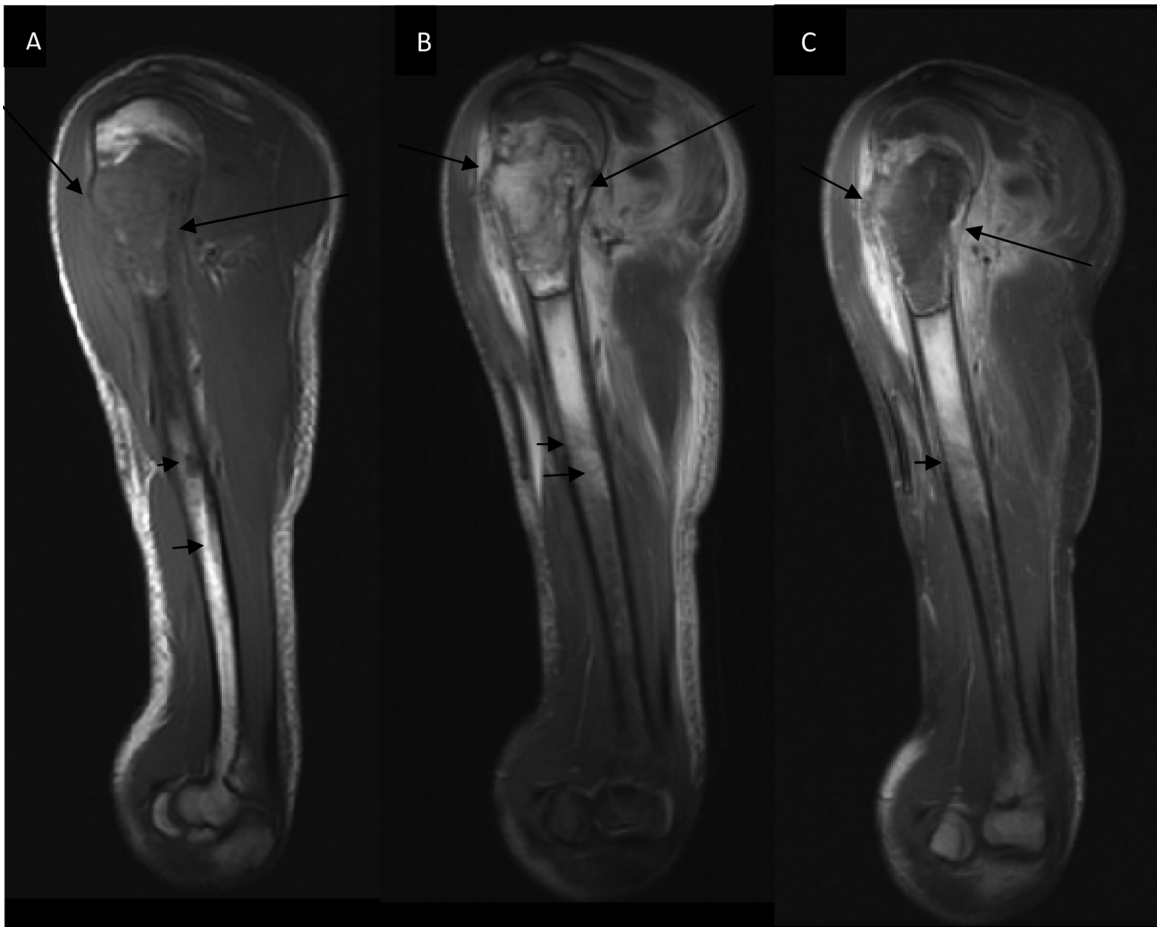

Figure 1. Skip lesions

15-year-old boy with osteosarcoma (arrows) right humerus at diagnosis. Sagittal mid-humeral MR images with (a) non-contrast T_1-weighted, (b) STIR (short tau inversion recovery) and (c) post-contrast fat saturated T_1-weighted sequences. Note mid-humeral diaphyseal focus of tumor (arrowheads), histologically proven to be a skip metastasis. This lesion is most inspicuous on non-contrast T_1-weighted sequence and becomes in distensible from adjacent edema in STIR sequenced. With contrast enhancement, the skip lesion becomes intense with enhancing edema.

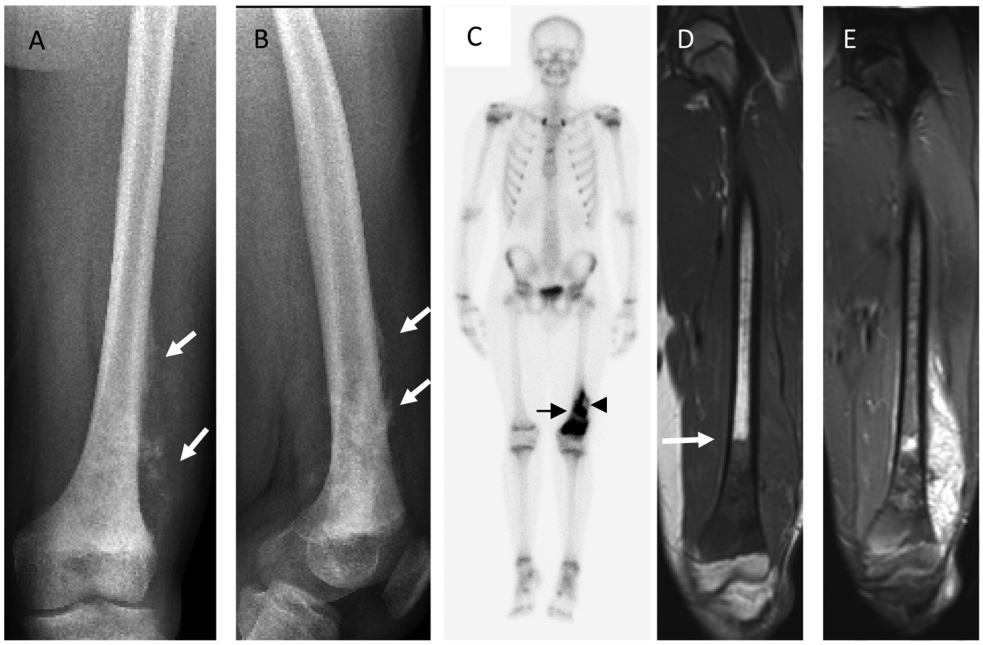

Figure 2. 16 year-old boy with osteosarcoma distal left femur; intramedullary tumor extent best shown on T_1-weighted sequence

A. Anteroposterior and B. lateral views of the left femur show aggressive periosteal reaction (arrows) distal left femur.

C. Coronal whole body ^{99m}Tc. MD P bone scan shows intensive metabolic activity within the intramedullary portion of the tumor (arrows) but relative paucity around the periphery of the extra cortical extent laterally (arrowhead).

D. Coronal non-contrast T_1 – weighted MR sequence exquisitely demonstrates the intramedullary extent of disease. The arrow indicates the sharp transition from normal bright fatty marrow to dark tumor marrow. Arrowheads delineate the soft tissue portion of disease.

E. With contrast administration, the soft tissue mass becomes well-delineated but the intramedullary transition enhances intensely with marrow enhancement.

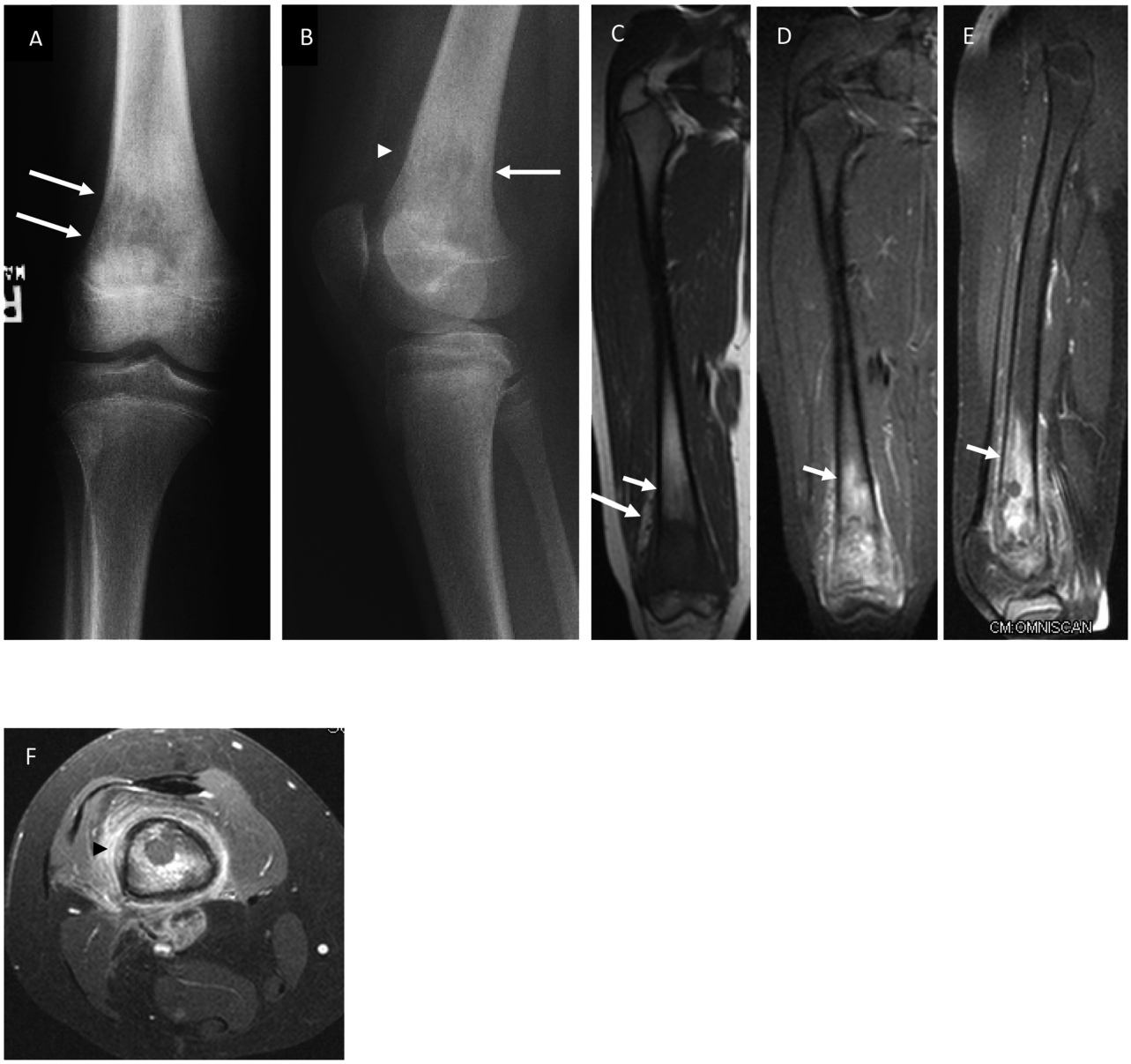

Figure 3. 13 year-old girl with 3 month history of right knee pain, histologically proven to be Ewing's Sarcoma

Anteroposterior, A, and lateral, B, radiographs of the right knee show a poorly defined, irregular region of metaphyseal demineralization (arrows) with minimal anterior cortical scalloping, B (arrowhead). C, Coronal non-contrast T_1-weighted MR shows the intramedullary line of demarcation of the tumor (long arrow) with mild adjacent poorly defined intramedullary edema (short arrow). Coronal STIR, D, and sagittal post-contrast T_1-weighted image with fat suppression demonstrate the extent of the intramedullary enhancing edema (short arrows). On these two sequences, the increased signal of the edema silhouettes the intramedullary tumor making delineation of tumor from surrounding edema difficult. The axial post-contrast T_1-weighted image with fat saturation, F, confirms these findings but also shows tumor extension through the medial cortex (black arrowhead). Note the

similarities in the appearance of the radiographs, soft tissue and intramedullary edema in this case with those in Figure 4.

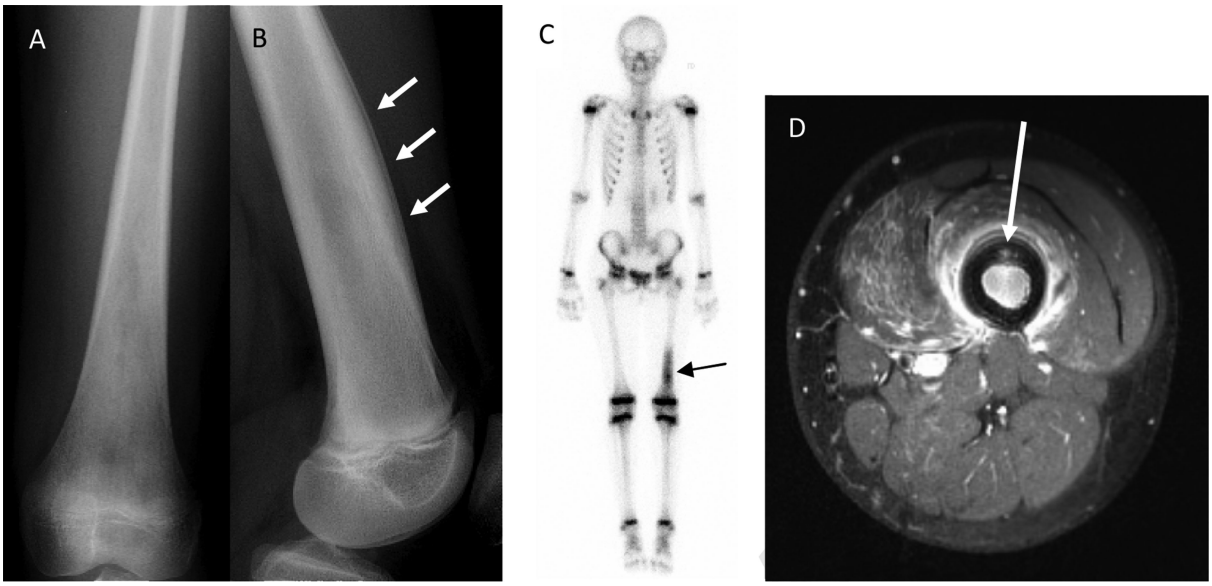

Figure 4. 9-year-old girl underwent evaluation for left thigh pain of several weeks duration with presumed diagnosis of Ewings sarcoma family of tumors

A. Anteroposterior and B. lateral radiographs of the left femur demonstrate subtle heterogeneous mineralization and layered periosteal reaction along the anterior diaphysis (arrows). These findings correlate with increased metabolic activity shown on the corresponding ^{99m}Tc-MDP bone scan C. (arrow). Within the increased activity left distal femur is a focus of more intense activity (arrow). D. This focus correlates with the tiny cortical abscess demonstrated on axial contrast-enhanced MR (arrow) with fat saturation, indicative of osteomyelitis and confirmed by biopsy.

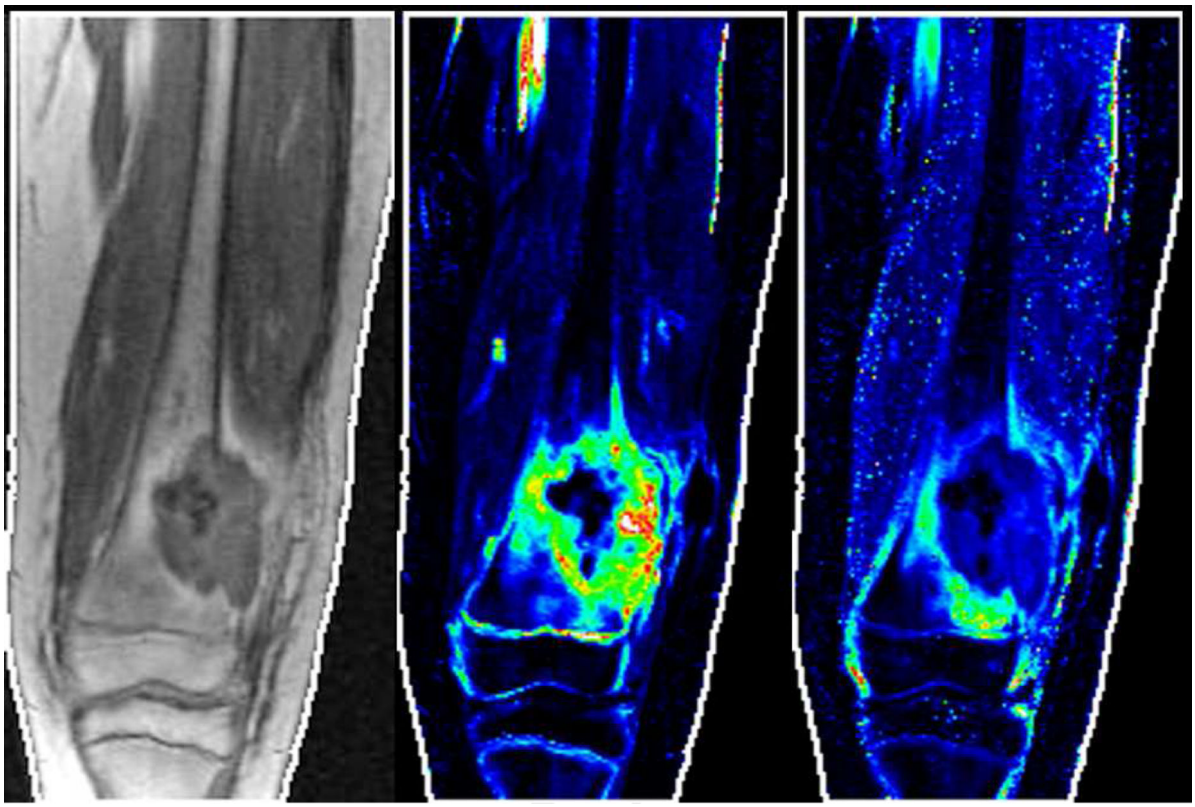

Figure 5. Dynamic enhanced MRI (DEMRI) (Courtesy of Wilburn E. Reddick, Ph.D.)

14-year-old female with osteosarcoma distal left femur at baseline evaluation.

The left-hand image is the final T_1-weighted contrasted enhanced dynamic set. Quantitative T1 relaxation measures before contrast middle image) and dynamic contrast-enhanced (DCE)-MRI (right-hand image) were both acquired as 16 slice 3D acquisitions with 5 mm thick sections covering the full extent of the tumor. A representative section from the center of the imaging volume is shown.the middle image is the Ktrans (transfer rate constant for contrast transfer from plasma to extracellular space) [min^{-1}] image. The right-hand image is ve (fractional extracellular / extravascular space).

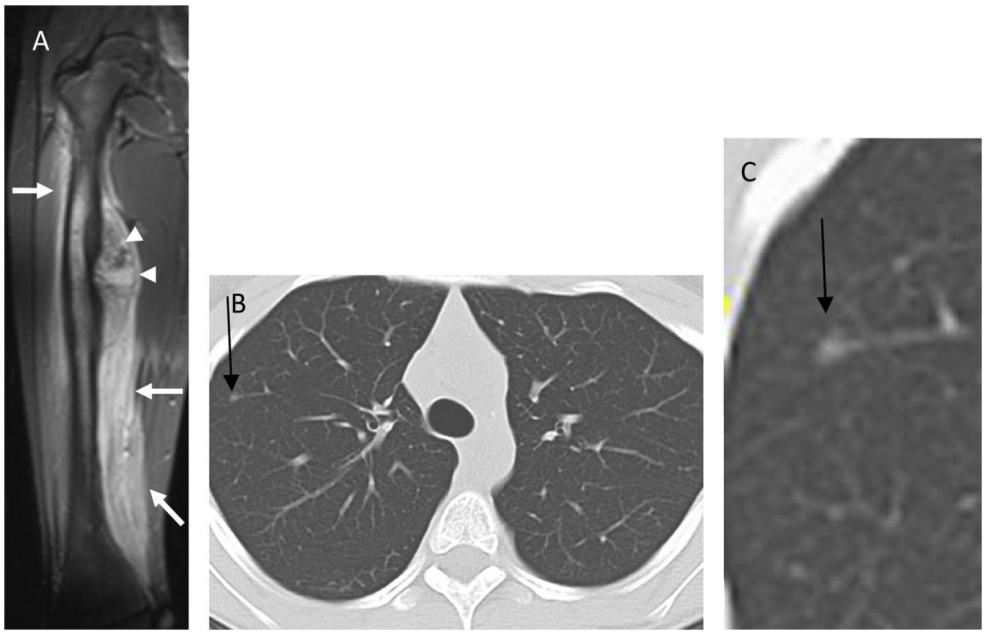

Figure 6. 14-year-old girl underwent evaluation of 2 month history of right thigh pain and swelling. She was diagnosed with high grade right femoral periosteal osteosarcoma (arrowhead)

A. The coronal STIR image of the right thigh demonstrates massive edema (arrows) extensively involving the adductor muscles and to a lesser extent, abductor muscles.

B. and C. Staging chest CT revealed a non-specific 4mm nodule in the right upper lobe (arrow) which was histologically proven to be acute necrotizing granuloma with bronchiolitis but no evidence of malignancy.

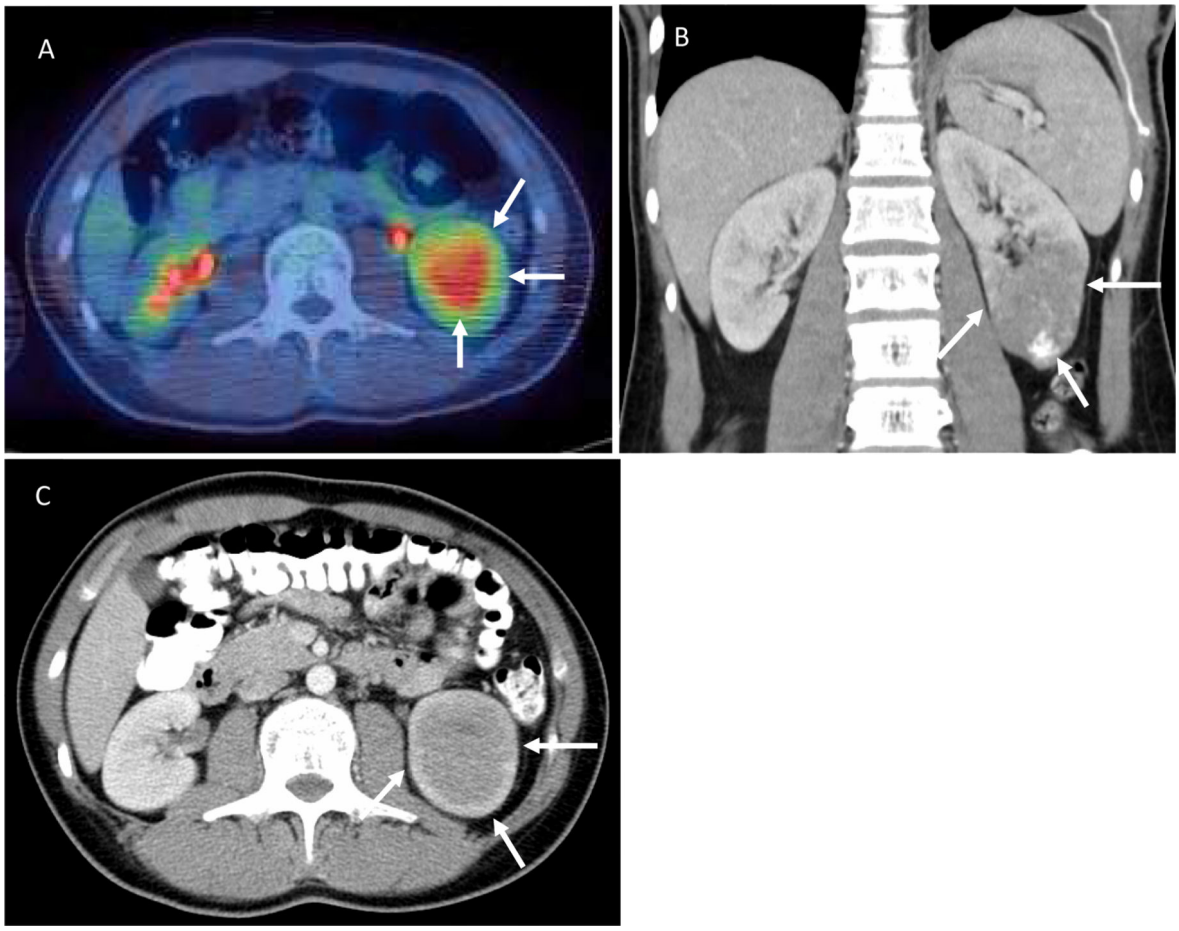

Figure 7. 18-year-old male treated 6 years earlier for osteosarcoma right tibia underwent surveillance PET-CT for monitoring of disease recurrence

A. Fused PET-CT image showing metabolically active metastatic osteosarcoma of the lower pole left kidney (arrows).

B. Coronal and C. axial reformatted images from a contrast-enhanced diagnostic abdominal CT scan shows the large left lower pole renal mass with tumor calcifications (arrows)

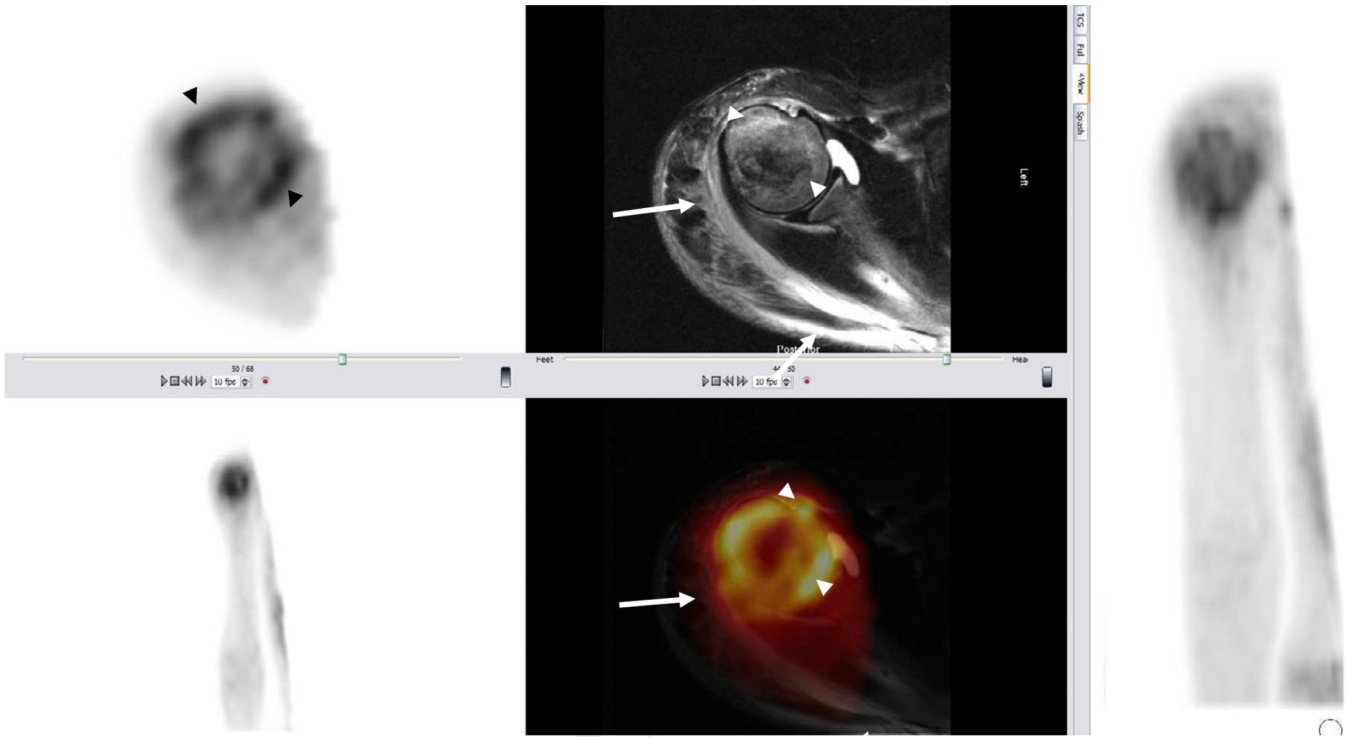

Figure 8. PET-MR right humeral osteosarcoma (Courtesy of Barry S. Shulkin, MD, MBA)

15 year-old with proximal right humeral osteosarcoma at time of diagnosis. Multiplanar PET-CT images through the right humerus and axial fat saturated T_2-weighted image through the proximal humeral osteosarcoma merged with a comparable image from reconstructed PET-CT study shows intense abnormal metabolic activity most prominent around the periphery of the tumor (arrowheads). Note relative absence of metabolic activity in the associated soft tissue edema (arrows).

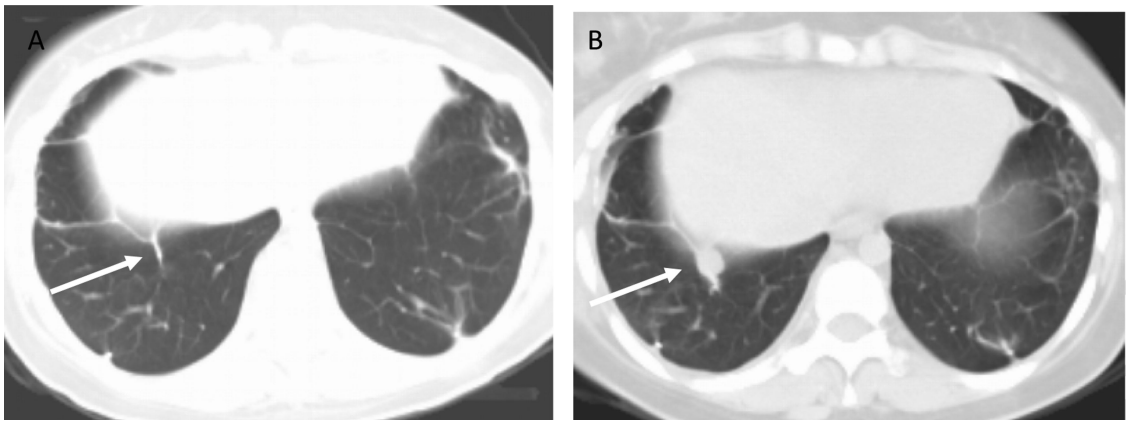

Figure 9.

Chest CT was performed 2 months after thoracotomy for pulmonary metastectomy, A, and revealed tumor recurrence in right lower lobe scar (arrow), B. Note nodular expansion within the scar. (Courtesy of M. Beth McCarville, MD)